Experiments in Fluids 17 (1994) 267–271 © Springer-Verlag 1994

Unexpected ricochet of spheres off water

D. J. Shlien

Abstract A sphere was observed to apparently ricochet off the free surface of water at incident angles as large as 45° while the expected (empirical/analytical) maximum angle to the horizontal for ricochet was 6°. Closer examination of the process revealed that the cavitating sphere penetrated the liquid to depths as great as 35 sphere diameters. Under certain circumstances the sphere was also observed to leave the liquid in a direction close to the incoming direction; that is, the sphere ricocheted backwards! This peculiar behavior was found to be a result of an unintentional spin applied to the sphere upon launching. By crudely modelling the process, the sphere path is qualitatively predicted. It was found that the drag and lift coefficients required to model the trajectory data were several times smaller than those obtained for the non-cavitating case or for the non-spinning case. If more precise sphere trajectory data were available, this experiment could be used to measure the lift and drag coefficients of a spinning and cavitating sphere.

1 Introduction

The phenomenon of ricochet of a sphere off the free surface of water was well known from at least the time of the Battle of Trafalgar, 1805, when the range of ship-mounted cannons was increased by aiming the ball so that it would ricochet off the sea surface. In addition to extending the range, the cannon ball would be more likely to inflict damage on its target due to the lower trajectory. Extensive tests were performed in 1838 (reported by Johnson and Reid, 1975) in which a 54 lb cannon ball was observed to ricochet over 30 times! Ricocheting was also used by the British in WWII with the "bouncing bomb" plan of Barnes Wallis to destroy the Möhne Dam in Germany. This was discussed in the biography of Barnes Wallis by Morpurgo (1972).

Received: 6 September 1993 / Accepted: 15 February 1994

D. J. Shlien
Saginaw Valley State University, University Center, Michigan 48710, USA

The author would like to thank T. Miloh for suggesting an experimental investigation into the ricochet problem and for his help and discussion of this work. Preliminary experiments were performed by Jim Oelberg as a special undergraduate project. Randy Hostetler, our Laboratory Supervisor, designed and built the final apparatus and John Leonard our Instrument Repair Technician, built and improved the associated electronic equipment for the timing device.

The maximum incident angle for ricochet to occur can be estimated by the empirical result:

$$\text{critical angle} = 18°/(\text{projectile specific density})^{1/2} \quad (1)$$

The source of this relationship is discussed in a fascinating review of the subject of the ricochet phenomenon by Johnson and Reid (1975). Wallis' design involved applying a back-spin (peripheral to translational velocity ratio of 0.3) to the bomb to increase the critical angle for ricochet. He carried out a series of experiments for his design, but unfortunately his original data were accidentally destroyed. Hutchings' (1976) analysis of a spinning cylindrical projectile resulted in an additional term in the cylindrical form of the empirical equation, Eq. (1). A significant increase in critical angle was observed, due to an applied back-spin. No references were found which mentioned the possibility of a spinning projectile fully submerging before exiting the liquid.

This work was undertaken in an attempt to verify the analysis of Miloh and Shukron (1991). The results of the latter analysis reduced to Eq. (1) when the Froude number is large. Thus the work to be presented here deals with the ricochet phenomenon at relatively high velocities.

Equation (1) results in a critical angle of 6° for a steel sphere. Thus, in a preliminary investigation of this phenomenon, it was most surprising to find that ricochet occurred at approach angles to the free surface of 30° and even 45°. In addition, in one case the sphere even ricocheted backwards! When the experiment was set up, it was thought that the spin introduced by the propulsion method would be small and that its effect would similarly be small. Here, the investigations shall be presented and it will be shown that the observed phenomena can be qualitatively reproduced by analysis.

2 Apparatus

The experiments were performed in a channel 30 cm wide, 46 cm deep and over 2 m long. Water was filled to a depth of 31 cm. The motion of the sphere was recorded on video tape and played back by single stepping each field.

The propulsion apparatus consisted of an 80 ml reservoir of compressed air (normally 690 kPa), a solenoid activated valve which separated the compressed air from the 0.635 cm sphere, and 75 cm long polyethylene tube (Fig. 1). The tube was directed to a set angle from the water free surface. The end of the tube was approximately 9 cm above the water surface. The solenoid valve was then opened to propel the 0.635 cm

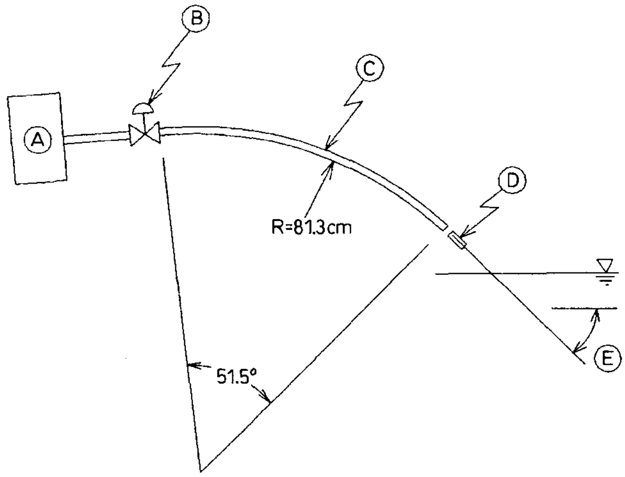

Fig. 1. Sphere propulsion apparatus. *A* air reservoir; *B* solenoid actuated valve; *C* polyethylene tube; *D* sphere speed measurement device; *E* adjustable angle, 30° to 45°

sphere through the polyethylene tube. The sphere speed was measured by the time interval the sphere interrupted two light beams spaced 5.04 cm apart along the trajectory. This timing apparatus was placed at the tube exit.

3
Observations

Two sequences of successive video fields, showing the sphere trajectory, are reproduced in Fig. 2. For both of these cases, the incident angle is 45° and the sphere diameter is 0.635 cm. The scale of the photograph may be determined from the 6 inch ruler positioned horizontally just above the water surface. The sphere path is made visible by the trial of cavitation bubbles. The initial impact splash is evident in sequence (a) in which the steel sphere can be seen to exit at an angle of 65°. (Notice that part of the path of the exiting sphere in air can be seen in both sequences as a short streak.) In sequence (b), the exit angle of the acrylic sphere is 110°. This unexpected behavior can only be attributed to spin of the sphere.

In these experiments, the launch tube was set up as shown in Fig. 1. In a subsequent experiment, the sign of curvature of the tube was reversed, that is, instead of the launch tube being concave down, it was manipulated to be predominately concave up. The path of the sphere was then observed to deviate downwards from the straight line path instead of upwards. It may thus be concluded that the unexpected observations were a result of spin of the sphere, since the modified curvature direction of the launch tube changed the spin direction of the sphere.

4
Analysis

The observations can be modelled simply if the splash and the energy lost upon impact are neglected. The equations of motion of the sphere are obtained by equating the product of the sphere mass m_s, times its acceleration to the vector sum of all of the forces exerted on the sphere. These forces consist of the force W of gravity on the sphere, the buoyancy force B (weight of the displaced fluid), the drag force D, and the lift force L. The magnitudes D and L are written in terms of the drag and lift coefficients, C_D and C_L respectively: $D = C_D A \frac{1}{2}\rho_f V'^2$ and $L = C_L A \frac{1}{2}\rho_f V'^2$ where $A = \pi d^2/4$, is the sphere diameter, ρ_f is the fluid density and $V' = (u'^2 + v'^2)^{1/2}$ is the magnitude of the sphere velocity, in which u' and v' are the x (horizontal) and y (vertical) components of the sphere velocity. The horizontal and vertical component equations are thus:

$$m_s \frac{du'}{dt'} = D_x + L_x \tag{2}$$

$$m_s \frac{dv'}{dt'} = D_y + L_y + (B - W) \tag{3}$$

where t' is time and subscripts x and y denote horizontal and vertical components, respectively. Substituting the given expressions for D and L results in:

$$\frac{du'}{dt'} = -\left(C_D \frac{u'}{V'} + C_L \frac{v'}{V'}\right) \frac{3}{4} \frac{\rho_f}{\rho_s} \frac{V'^2}{d} \tag{4}$$

$$\frac{dv'}{dt'} = \left(-C_D \frac{v'}{V'} + C_L \frac{u'}{V'}\right) \frac{3}{4} \frac{\rho_f}{\rho_s} \frac{V'^2}{d} - \left(1 - \frac{m_f}{m_s}\right) g \tag{5}$$

The equations are then made dimensionless by defining the following dimensionless variables: $u = u'/V'$, $v = v'/V'$, $t = t'V'/d$ and $V = V'/V_0$, where V_0 is the velocity V' at the initial time $t = 0$. This results in the following form of the equations of motion:

$$\frac{du}{dt} = -(C_D u + C_L v) \frac{3}{4} R \tag{6}$$

$$\frac{dv}{dt} = (-C_D v + C_L u) \frac{3}{4} R - \frac{b}{V^2} \tag{7}$$

where $R = \rho_f/\rho_s$, the ratio of the density of the fluid to that of the solid, and $b = (1 - R) g d / V_0^2$, the net buoyancy factor.

The equations of motion can be solved for the sphere trajectory, providing the initial velocity and expressions for C_D and C_L are given. Unfortunately no data are available for drag and lift of spinning and cavitating spheres. Therefore an attempt was made to fit equations for C_D and C_L to obtain the observed trajectory. It will be seen that the trajectory resulting from the analysis does qualitatively exhibit the observed behavior but limited success was achieved in reproducing the measured trajectory in all cases. It is to be noted that the main purpose of the analysis is to explain and to qualitatively predict the observed behavior, rather than to obtain accurate expressions for the drag and lift coefficients. The latter objective requires more detailed data.

5
Drag and lift coefficients

The model will be compared with observations of a 0.635 cm diameter steel sphere at a speed of approximately 75 m/s and ratio of peripheral velocity to translational velocity of 0.9, with two different incident angle: 30° (Run A) and 45° (Run B). Under these conditions the cavitation number $Ca = (p - p_v)/(\frac{1}{2}\rho_f V'^2) = 0.035$, confirming that the bubbles observed in Fig. 2 are indeed due to cavitation. Here $(p - p_v)$ is the difference between the pressure of the undisturbed fluid and the fluid vapor pressure.

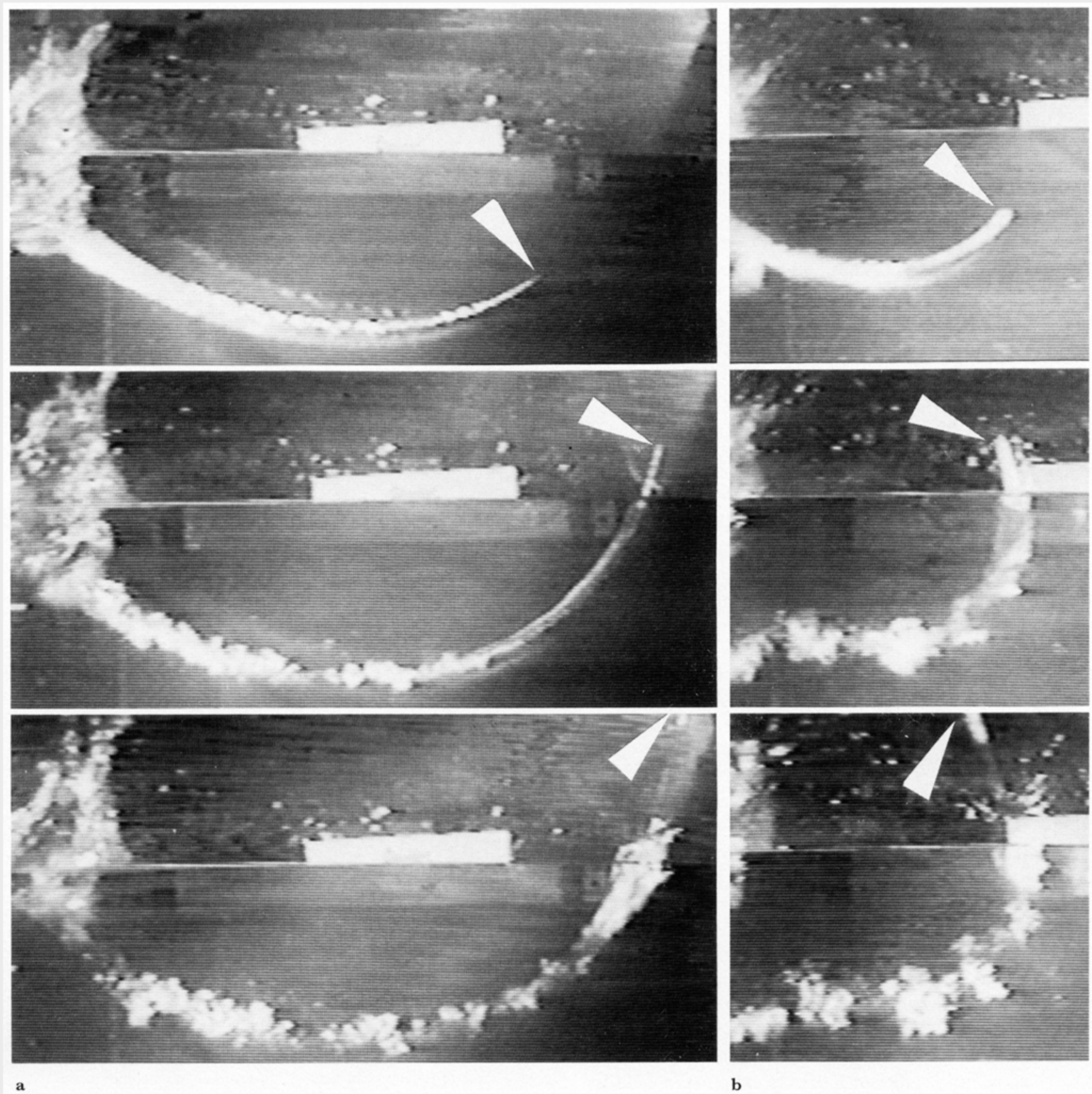

Fig. 2a, b. Two sequences of successive video fields showing the sphere trajectory with incident angle of 45°. The time interval between fields is 1/60 s. Sequence **a**: steel sphere, sequence **b**: acrylic sphere. Arrow heads indicate sphere position

The ratio of peripheral to translational sphere velocity U'/V' was estimated from an expression by Barkla and Auchterlonie (1971) in terms of the total bend angle of the tube α, and the coefficient of friction μ, between the sphere and tube wall:

$$\frac{U'}{V'}=\frac{5}{2}\mu\alpha \tag{8}$$

This expression was obtained from the ratio of (moment × time)/(moment of inertia). By bonding two spheres together and measuring the angle at which they first slip within the tube, μ was found to be approximately 0.4. The angle $\alpha=51°$ yields $U'/V'=0.9$ and thus a spin rate of 3300 rev/s! This high spin rate would certainly be expected to affect the cavitation process and to influence the values of C_D and C_L.

Since, to the author's best knowledge, there are no published data for the drag coefficient of a cavitating spinning sphere, known values of C_D will be discussed for other cases. The range of Reynolds numbers observed here is from 35×10^3 to 520×10^3. For a non-spinning, non-cavitating sphere in a uniform flow,

C_D is essentially constant at 0.45. A value of $C_D = 0.7$ can be extracted from the work of Barkla and Auchterlonie for non-cavitating spinning spheres. Measured values of C_D for non-spinning spheres as a function of cavitation number in the Reynolds numbers range of 120×10^3 to 330×10^3 have been reported by May (1975). A trend of increasing C_D with increasing Reynolds number was observed but the reported data scatter was considerable. For $Re = 490 \times 10^3$ and cavitation number $Ca = 0.034$ (the conditions of Run A to be considered here), a drag coefficient of approximately 0.275 is reported. The drag coefficient will be assumed constant, for simplicity. However, as has been pointed out by Miloh (1993, private communication), for drag considerations, if the effective velocity of the bottom half of the sphere is assumed to be $V' + U'$ and that of the top half is $V' - U'$, the total drag force is proportional to $V'^2 + U'^2$ if the drag on the two parts is regarded to be independent.

Just as there are no data available for the drag of a cavitating and spinning sphere, no data were found for the lift coefficients. Although potential theory for a spinning cylinder yields a lift coefficient proportional to the ratio of peripheral velocity to translational velocity, the Magnus or Robins effect, measurements yield a nonlinear variation. Barkla and Auchterlonie presented their indirect measurements of C_L for a non-cavitating spinning sphere together with those of Maccoll (1928) as a function of the ratio of peripheral to translational velocities, U'/V'. For simplicity, it is assumed here that C_L for the cavitating spinning sphere depends upon this ratio in one of two ways: (a) the lift coefficient is constant or (b) it is inversely proportional to V, the dimensionless translational velocity of the sphere, $C_L = k/V$. Here k is the constant of proportionality and represents the initial value of C_L; i.e., the value of C_L when $V' = V_0$. The first method (a), assumes that the peripheral velocity decreases with time at the same rate as the translational velocity while (b) assumes that the change in peripheral velocity U', is small compared with the change in translational velocity, V'. Since the dimensionless value of V', V, is initially unity and decreases with time, assumption (b) results in C_L increasing with time. Using the calculation methods and the data from Barkla and Auchterlonie for Run A, the ratio of peripheral to translational sphere velocity was estimated to be 0.9, yielding a lift coefficient of 0.33. Since this result is for non-cavitating spheres, the actual lift coefficient for the present experiment is expected to be different from this estimate.

Thus, for Run A, it is initially estimated that $C_D = 0.275$ (from cavitating but non-spinning data) and that $k = 0.33$ (from spinning but non-cavitating data). Here it is assumed that the magnitude of the sphere's initial velocity V_0, and its angle of entry are known. What is actually measured is the velocity and angle with which the sphere leaves the launching apparatus: the effect of the entry splash and the effect of the propelling air blast are considered negligible. To summarize, the main assumptions of the analysis are: negligible effect of splash and air blast of the entering sphere, constant value of C_D, and either variation (a) or (b) of C_L with dimensionless velocity V.

6
Results and discussion

The equations of motion, Eqs. 6 and 7, were solved by a finite difference method. A step size of one sphere diameter was found to yield sufficiently accurate results. The measured trajectory was determined from the position of the cavitation bubble recorded on video tape (similar to the photos in Fig. 2). Path points extracted from the video tape of Run A (0.635 cm steel sphere at 76.5 m/s at 30°) are plotted in Fig. 3a together with the calculated trajectory, using $C_L = k/V$, in accordance with assumption (b). As expected, the values of $k = 0.33$ and $C_D = 0.275$ suggested by the references (previously discussed) clearly do not fit the data. A close fit to the data is obtained by trial and error using $k = 0.037$ and $C_D = 0.075$. Figure 3a also shows the significant effects on the trajectory of a slight variation in k while Fig. 3b shows the effect of varying the value of C_D.

The result of assuming a constant value for C_L [assumption (a)] as applied to Run A is shown in Fig. 4. It can be seen that the lift force becomes too small to overcome gravity when using this assumption. Thus it may be concluded that the

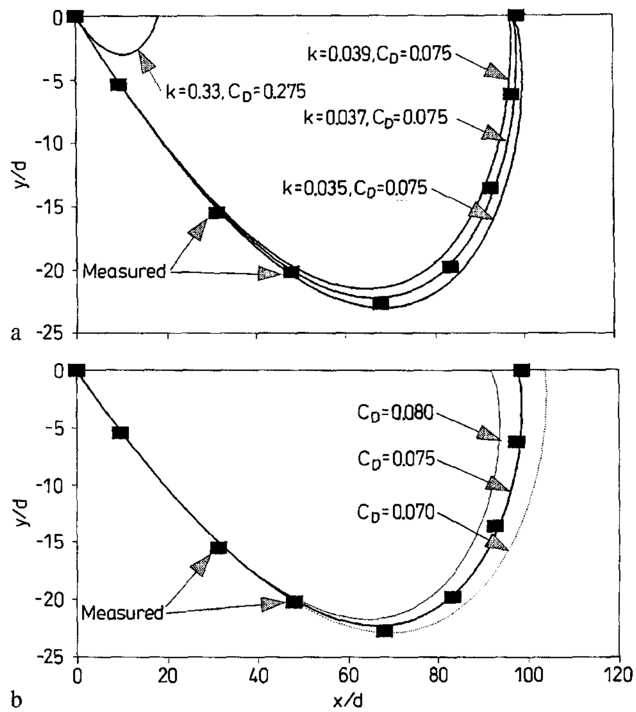

Fig. 3a, b. Sphere trajectory for Run A (76.5 m/s at 30° incident angle) compared with analysis assuming $C_L = k/V$. **a** Effect of varying k; **b** effect of changes in C_D

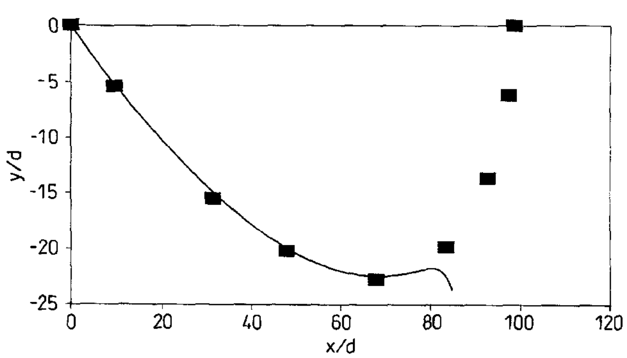

Fig. 4. Sphere trajectory for Run A compared with the analysis, assuming constant C_L

peripheral velocity of the sphere decreases more slowly than its translational velocity.

A verification of the fitted form for C_D and C_L was next attempted by comparison with measurements at sphere incident angle of 45° (Run B). For assumption (b), $C_L = k/V$, it can be seen in Fig. 5a that the lift coefficient increases too rapidly resulting in a curl in the sphere path. The fit does not improve much if the values of k and C_D are changed. If a constant value of lift coefficient [assumption (a)] is taken, Fig. 5b shows that the lift force becomes too small and thus the sphere does not leave the liquid. If a larger value of C_L is assumed, the calculated trajectory deviates excessively from the measured trajectory. It may be concluded that the assumed form for C_L should lie between a constant and k/V, say $C_L = k/V^a$ where a is a positive parameter less than 1. This latter fit was applied to Run B, but little improvement over the previous attempts was found.

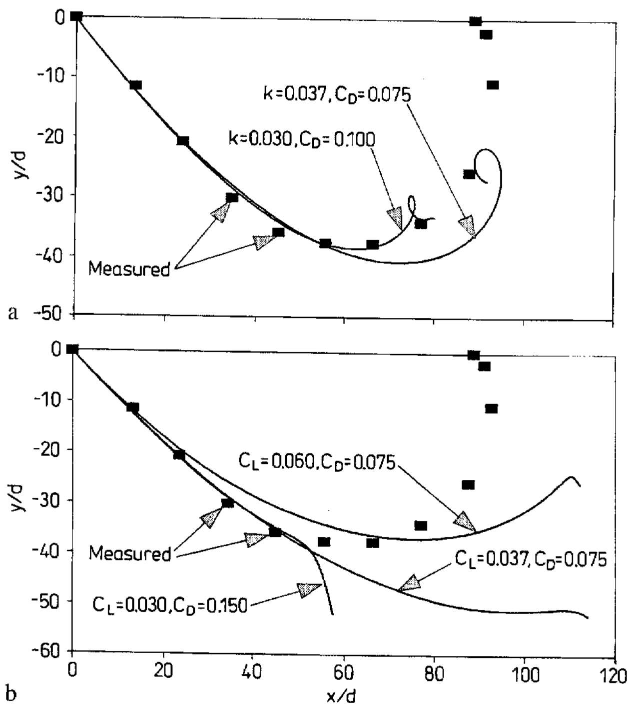

Fig. 5a, b. Sphere trajectory for Run B (81.9 m/s at 45° incident angle) compared with analysis. **a** Analysis assuming $C_L = k/V$; **b** assumes constant C_L

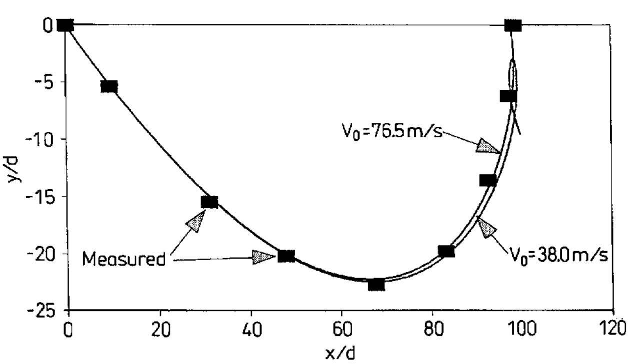

Fig. 6. Effect of initial velocity V_0 on sphere trajectory for Run A with $C_L = 0.037/V$ and $C_D = 0.075$. The curve for $V_0 = 150$ m/s coincides with that for $V_0 = 76.5$ m/s

The present analysis neglects the energy loss due to impact splash. Such an energy loss can be considered to result in a decreased initial velocity of the sphere, V_0. As can be seen from the equations of motions, Eqs. (6) and (7), a change in V_0 only affects the magnitude of the buoyancy factor b. The term involving b is usually small compared with the remaining terms except when the lift force is small as seen in Fig. 4. In Fig. 6, it can be seen that a large change in V_0 results in a small change in the sphere trajectory for Run A with $C_L = 0.037/V$ and $C_D = 0.075$. Similar small effects were observed for Run B and for the constant C_L case. Thus it may be concluded that the effect on the sphere trajectory due to initial energy losses is small.

7
Summary and conclusions

Before the present observations it was generally assumed that a spherical projectile (spinning or non-spinning) would either be propelled into a liquid or ricochet off the free surface of the liquid. It has been shown here that there is a third possibility: the sphere may enter the liquid, become submerged to a depth of as great as 35 sphere diameters, and then leave the liquid at an angle greater than its entry angle! This includes the case of the sphere leaving at an angle greater than 90°, that is, having a horizontal component of velocity in the direction from which it came.

The analysis was compared with the measured trajectories at Reynolds number of about 0.5×10^6, cavitation number of 0.035, ratio of peripheral to translational sphere velocity $U'/V' = 0.9$ and two entry angles of 30° and 45°. For both entry angles, $C_D = 0.075$ appeared to fit well with the data. For the 30° case, $C_L = 0.037/V$ resulted in a fit within the accuracy of the data, while assuming C_L = constant did not yield a sphere exiting trajectory. For the 45° entry case, neither C_L = constant nor $C_L = k/V$ gave a complete trajectory. A variation of C_L with V between these two cases, i.e. $C_L = k/V^a$ with $0 < a < 1$, did not significantly improve the data. The drag and lift coefficients used in the model were several times smaller than those reported by others for the non-cavitating or for the non-spinning cases. The effect of the entry splash on the trajectory is small.

High speed photography could yield the sphere position as a function of time. If the data are accurate enough to extract the components of the sphere instantaneous acceleration, the equations of motion, Eqs. 5 and 6, could be solved for the lift and drag coefficients. Thus, these observations could be used to measure the drag and lift coefficients of spinning, cavitating spheres.

References

Barkla HM; Auchterlonie LJ (1971) The Magnus or Robins effect on rotating spheres. J Fluid Mech 47: 437–447

Hutchings IM (1976) The ricochet of spheres and cylinders from the surface of water. Int J Mech Sci 18: 243–247

Johnson W; Reid SR (1975) Ricochet of spheres off water. J Mech Eng Science 17: 71–81.

Maccoll JW (1928) Aerodynamics of a spinning sphere. J Roy Aero Soc 32: 777–797

May A (1975) Water entry and the cavity-running behavior of missiles, Ch. 2. SEAHAC/TR 75-2, Naval Surface Weapons Center, White Oak Lab, White Oak, Silver Spring, MD

Miloh T; Shukron Y (1991) Ricochet off water of spherical projectiles. J Ship Research 35: 91–100

Morpurgo JE (1972) Barnes Wallis, A Biography, Longman, London